FEBS Letters 579 (2005) 2788–2794 FEBS 29543

NMR structure and regulated expression in APL cell of human SH3BGRL3

Chao Xu[a,1], Peizheng Zheng[b,d,1], Shuhong Shen[b], Yingqi Xu[a], Ling Wei[c], Hengjun Gao[c], Shengnian Wang[c], Chongri Zhu[c], Yajun Tang[a], Jihui Wu[a], Qinghua Zhang[b,c,*], Yunyu Shi[a,*]

[a] *Hefei National Laboratory for Physical Sciences at Microscale, School of Life Sciences, University of Science and Technology of China, Hefei 230026, PR China*
[b] *State Key Laboratory of Medical Genomics, Shanghai Institute of Hematology, Ruijin Hospital, Shanghai Second Medical University, Shanghai 20025, PR China*
[c] *National Engineering Center for Biochip at Shanghai, Shanghai 201203, PR China*
[d] *Department of Clinical Laboratory, Union Hospital, Fujian Medical University, 29 XinQuan Road, Fuzhou, Fujian 350001, China*

Received 3 February 2005; revised 4 April 2005; accepted 4 April 2005

Available online 20 April 2005

Edited by Christian Griesinger

Abstract SH3 domain binding glutamic acid-rich protein like 3 (SH3BGRL3) is the new member of thioredoxin (TRX) super family, whose posttranslational modified form was identified as tumor necrosis factor α (TNF-α) inhibitory protein, TIP-B1. In this paper, we determined its solution structure by multi-dimensional nuclear magnetic resonance spectroscopy. The overall structure of human SH3BGRL3 conformed to a TRX-like fold. To understand its function in vivo, the upregulated expression in acute promyelocytic leukemia cell line NB4 at both mRNA and protein level was elucidated. Immunofluorescence and immunohistochemistry staining with monoclonal antibody against SH3BGRL3 demonstrated that it was a cytoplasmic protein in both NB4 cell and human tissues. These results, as a whole, indicate that SH3BGRL3 may function as a regulator in all-*trans* retinoic acid-induced pathway.

Keywords: SH3 domain binding glutamic acid-rich protein like 3; Nuclear magnetic resonance structure; Leukemia; All-*trans* retinoic acid; Differentiation; Localization

1. Introduction

Human SH3BGRL3 (SH3 domain binding glutamic acid rich like protein 3) is a gene identified recently and mapping to 1p34.3–35 [1], which belongs to thioredoxin (TRX) super family. SH3BGRL3 codes for a highly conserved small functionally uncharacterized protein consisting of 93 amino acids. Like other two family members SH3BGRL [2] and SH3BGRL2 [3], SH3BGRL3 protein is homologous to N-terminal region of SH3BGR protein. However, lacking the conserved SH3-binding motif, which exists in SH3BGR and could also be found in SH3BGRL and SH3BGRL2, implied that the function of SH3BGRL3 should be quite different from these three proteins. Sequence of SH3BGRL3 shows a significant similarity to glutaredoxin 3 of *Escherichia coli*, but it completely lacks the conserved consensus sequence (CXXC), which is essential for glutaredoxin enzymatic activity [1]. The sequence of SH3BGRL3 is as same as that of C-terminal domain of tumor necrosis factor α inhibitory protein (TIP-B1), a TNF-α inhibitory protein identified, purified, and characterized from cytosolic extracts of TNF-treated human fibroblasts [4]. TIP-B1 protects cells from apoptotic lysis induced by TNF-α after they were pre-incubated with TIP-B1 [4–7]. Another study revealed that the SH3BGRL3 gene expression is up regulated in HL60 cells associated with the differentiation induced by phorbol–myristate–acetate (PMA) [8]. These suggested that the SH3GRL3 might function in the differentiation related signal transduction pathway networks.

Acute promyelocytic leukemia (APL) is a specific type of acute myeloid leukemia characterized by the t(15; 17) translocation that fuses the *PML* gene to the retinoic acid receptor α (RARα) gene on chromosome 17 to form the fusion gene and leukemogenic protein PML-RARα. It has been demonstrated that PML-RARα inhibits all-*trans* retinoic acid (ATRA)-induced differentiation and contributes to leukemogenesis and that ATRA could induce the degradation of PML-RARα, and rescue the blocked differentiation in APL [9].

Since the function of SH3BGRL3 remains obscure, in this paper, we report the solution structure of human SH3BGRL3 and speculate the potential binding sites by backbone relaxation experiments. Structure comparison with other known structures reveals that it belongs to TRX superfamily, and its structure is similar to glutaredoxin 3 of *E. coli* [10] and PICOT homology domain 2 of PICOT [11]. We also report the regulated expression with ATRA in APL cell line NB4 at both mRNA and protein level. Our results suggest that SH3BGRL3 may function as a regulator rather than an enzyme in the ATRA-induced pathway.

*Corresponding authors.
E-mail addresses: qhlzhang@sh163.net (Q. Zhang), yyshi@ustc.edu.cn (Y. Shi).

[1] These authors contribute equally to this paper.

Abbreviations: SH3BGRL3, SH3 domain binding glutamic acid-rich protein like 3; APL, acute promyelocytic leukemia; ATRA, all-*trans* retinoic acid; TNF-α, tumor necrosis factor-α; PMA, phorbol–myristate–acetate; HRP, horseradish peroxidase; NMR, nuclear magnetic resonance; PAGE, polyacrylamide gel electrophoresis; TRX, thioredoxin; TIP, TNF-α inhibitory protein; GAPDH, glyceraldehyde 3-phosphate dehydrogenase

0014-5793/$30.00
doi:10.1016/j.febslet.2005.04.011

2. Materials and methods

2.1. Cell culture and treatment

Retinoid acic (RA)-sensitive NB4 cells were cultured under conditions previously described [9,12]. The in vitro culture contained 1 μmol/L ATRA. Total RNAs were extracted at indicated time-points using the Trizol reagent (Invitrogen Inc.) and quality controlled with Bioanalyzer 2100 capillary electrophoresis (Agilent) prior to the following experiment. Cell differentiation was evaluated by cell morphology changes using Wright's staining, CD11b expression, and the nitroblue tetrazolium reduction test.

2.2. cDNA microarray

A set of three slides cDNA microarrays covering 12 630 genes was made in Shanghai Biochip and Shanghai Institute of Hematology. The 40 μg total RNA was labeled with Cy3-(non-treated) or Cy5-(treated) dCTP (Amersham Biosciences) as reverse transcription incorporation. The 50 pmol of fluorescence of labeled cDNAs was used as probe for hybridization and GenePix 4000B fluorescence scanner (Axon Inc.) was applied in scanning. The ImageQuant (Amersham Biosciences) and GeneSpring (Silicon Genetics) softwares were applied to analyze the expression of proper genes, and the normalization was based on expression level over the whole slides [13].

2.3. Real-time RT-PCR

The expression alteration of the SH3BGRL3 gene was further validated with real-time RT-PCR. The first strand cDNA was prepared with TaqMan® Reverse Transcription Reagents (Applied Biosystems, Foster City, CA). The primers were designed with PrimerExpress software (Applied Biosystems) and synthesized locally: F-5′AGAGCGAGGTGACCCGAAT, R-5′TGCCAAGGCTCGCATCTC. The GAPDH gene was used as internal control to calculate expression level with the primers: F-5′GAAGGTGAAGGTCGGAGTC, R-5′GAAGATGGTGATGGGATTTC. Real-time PCR was carried out in an iCycler iQ Real-Time PCR Detection system (Bio-Rad) using SYBR® Green I (Applied Biosystems) as the detection format. Amplification was carried out in a total volume of 25μl containing 1 × SYBR® Green I, 100 nM each primer, 10 nM calibration dye (Bio-Rad) and 2μl of 1:2 diluted cDNA. The thermal profile consisted of a 10 min of *Taq* polymerase activation at 95 °C, followed by 40 cycles of PCR at 95 °C for 15 s, 60 °C for 1 min. At the end of the PCR, the temperature was increased 0.5 °C every 10 s from 60 to 95 °C, and the fluorescence was measured every 10 s to construct the melting curve. A non-template control was run with every assay, and all determinations were performed at least in duplicates to achieve reproducibility.

2.4. Recombinant protein expression and purification

Human *SH3BGRL3* cDNA was obtained from human CD34+ hematopoietic stem/progenitor cell cDNA library, cloned in frame into pET-22 b (+) in the *Nde*I/*Xho*I sites (Novagen) with primers F-5′CAGGCTCACATATGAGCGGCCTGCG, R-5′CTGGGTTACTCGAGAGCCAGCTTCAGGAAC3′. The recombinant pET-22b-SH3BGRL3 vector was then transformed into *E. coli* strain BL21 (DE3) host cell for expression.

Recombinant human SH3BGRL3 was purified using Hitrap chelating column (Amersham Biosciences) chromatography. The purified recombinant protein consists of 101 amino acids, with a C-terminal His tag (-LEHHHHHH) carried over from the cloning vector. For the NMR studies, sample of purified doubly labeled protein was dissolved to a final concentration of 2 mM in 20 mM potassium phosphate (pH 7.0, containing 100 mM NaCl, 1 mM DTT, and 10% D_2O). For the amide proton exchange studies, protein was lyophilized and dissolved in D_2O.

2.5. NMR spectroscopy

All NMR experiments were performed on Bruker DMX500 and DMX600 spectrometers with self-shielded *z*-axis gradients at 295 K. The following spectra were recorded at 295 K to obtain backbone and side chain resonance assignments: 2D ^{1}H, ^{15}N-HSQC [14], 2D ^{1}H, ^{13}C-HSQC [14], 3D triple-resonance spectra HNCO [15], HN(CA)-CO [16], CBCA(CO)NH [17], CBCANH [18], C(CO)NH-TOCSY [19], H(CCO)NH-TOCSY [19], HCCH-TOCSY [20], HCCH-COSY [21], and HBHA(CBCACO)NH [22]. A complete assignment of aromatic side-chains was facilitated by the identification of aromatic d protons from 2D (HB)CB(CGCD)HD-COSY [23].

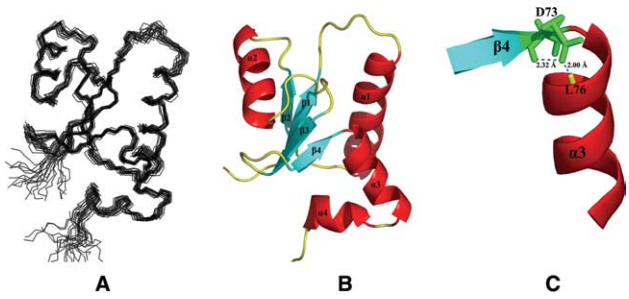

Fig. 1. Solution structure of human SH3BGRL3 protein. (A) Main chain representation of the 20 lowest energy structures superimposed on one another. (B) A schematic ribbon representation of SH3BGRL3. The helices are colored in red and strands are colored in cyan. (C) Two hydrogen bonds linking β4 to α3. The distances of OD1 of D73 and HN of D73 and L76 are marked.

Table 1
NMR structure determination statistics

Distance restraints	
Intraresidue ($i - j = 0$)	265
Sequential ($\|i - j\| = 1$)	353
Medium range ($2 < \|i - j\| < 4$)	355
Long range ($\|i - j\| > 5$)	351
Hydrogen bonds	22
Total	1346
Dihedral angle restraints[a]	
Φ	51
Ψ	51
Mean r.m.s.d[b] from the experimental restraints	
Distance	0.0131 ± 0.0002
Dihedral	0.1469 ± 0.0191
Mean r.m.s.d. from idealized covalent geometry	
Bond	0.0017 ± 0.00004
Angle	0.3208 ± 0.0023
Improper	0.1373 ± 0.0048
Mean energies (kcal mol^{-1})	
E_{total}	−450.66 ± 14.56
E_{vdw}	−293.51 ± 9.37
E_{NOE}	26.11 ± 1.76
E_{angle}	61.42 ± 2.29
E_{bond}	14.44 ± 1.74
$E_{improper}$	5.02 ± 0.39
$E_{dihedral}$	0.38 ± 0.13
PROCHECK Ramachandran plot analysis (%)[c]	
Residues in most favored regions	78.9%
Residues in additionally allowed regions	19.8%
Residues in generously allowed regions	0.5%
Residues in disallowed regions	0.8%
Structural r.m.s.d. to the mean coordinates[d] (Å)	
Backbone atoms (4–92)[d]	0.55
Heavy atoms (4–92)[d]	1.00

[a]The Φ and Ψ angle restraints are generated from secondary structures by CSI [24].
[b]r.m.s.d., root mean square deviation.
[c]All non-Gly residues; Φ/Ψ of most favored and additional allowed regions are given by program PROCHECK [32].
[d]The unstructured portions of the N- and C-terminal tails were not considered.

The chemical shift index (CSI) [24] was calculated for four types of nuclear: Cα, Cβ, C′, and Hα. The derived secondary structures based on the consensus CSI were converted into restraints on Φ and Ψ angles: for α-helix residues, Φ was limited in $-60 \pm 40°$ while Ψ was in $-50 \pm 50°$; for β-strand residues, Φ was limited in $-120 \pm 40°$ while Ψ was in $130 \pm 50°$. Hydrogen bond restraints were employed in areas of regular secondary structures, displaying characteristic NOE cross-peaks. Each deduced hydrogen bond was represented by two distance constraints: α-helix residues, 1.6–2.4 Å for HN–O and 2.4–3.3 Å for N–O; β-strand residues 1.4–2.7 Å for HN–O and 2.4–3.7 Å for N–O.

The distance information was collected by 3D ^{13}C separated and ^{15}N-separated NOESY [25] with 130 ms mixing times. NMR data processing was carried out using NMRPipe, and the data were analyzed with SPARKY version 3.106 [26]. Structures were calculated using the program CNS v1.1 [27], employing a simulated annealing protocol for torsion angle dynamics [28]. For the initial rounds of structure calculations, only sequential, intraresidual, medium-range NOEs, unambiguous long-range NOEs and dihedral angle restraints were used. Later, all other long-range NOEs and hydrogen bonds were introduced in consecutive steps. Simple impulsion non-bonded interactions were used during structure calculation. Twenty structures with the lowest total energy were selected to form a representative ensemble of the calculated structures.

2.6. ^{15}N relaxation experiments

All ^{15}N relaxation experiments were carried out at 295 K on a Bruker DMX500 NMR spectrometer. ^{15}N relaxation measurements were carried out using the published methods [29]. ^{15}N T_1 relaxation rates were measured with eight relaxation delays: 11, 62, 142, 243, 364, 525, 757, and 1150 ms. ^{15}N T_2 relaxation rates were measured with six relaxation delays: 17.6, 35.2, 52.8, 70.4, 105.6, and 140.8 ms. A recycle delay of 1 s was used for measurement of T_1 and T_2 relaxation rates. The spectra measuring ^{1}H–^{15}N NOE were acquired with a 2 s relaxation delay followed by a 3 s period of proton saturation. The spectra recorded in the absence of proton saturation employed a relaxation delay of 5 s. The exponential curve fitting and extract of T_1s and T_2s are processed by SPARKY [26].

2.7. Western blot, immunohistochemistry analysis and cellular localization

Western blot analysis. The ATRA treated NB4 cell lysates (~50 μg/sample) were separated by 15% Tris–SDS–PAGE (polyacrylamide gel electrophoresis) and transferred to Immobilon P membranes (Millipore) by electroblotting in 25 mM Tris–250 mM glycine–20% methanol (v/v) (4 °C, 90 V, 2 h). The purified P8E07 IgG3/κ isotype mcAb made with rh-SH3BGRL3 was used as primary antibody, and horseradish peroxidase (HRP)-labeled rabbit-anti-mouse antibody was as secondary antibody (Cell Signaling Technology), and the commercial anti-beta actin monoclonal antibody (Santa Cruz) was used to evaluate the protein loading amount. ECL kit (Cell Signaling Technology) was used to develop the results with X-ray film.

Immunohistochemistry. A tissue microarray including 46 normal representative paraffin embedded tissue samples from two accident available non-diseased human bodies was created with reported protocol [30] in Shanghai Biochip Center. Staining was revealed with P8E07 as primary antibody and HRP-conjugated secondary antibody using DAKO LASB+ kit (DAKO), following the manufacturer's instructions.

Cellular localization with immunofluorescence. The NB4 cell treated with ATRA for 48 h was applied for immunostaining as before [31], P8E07 to detect the SH3BGRL3, and FITC-labeled rabbit anti-mouse IgG was used as secondary antibody (Calbiochem). The images were taken with Axiovert 200 confocal microscope (Bio-Rad).

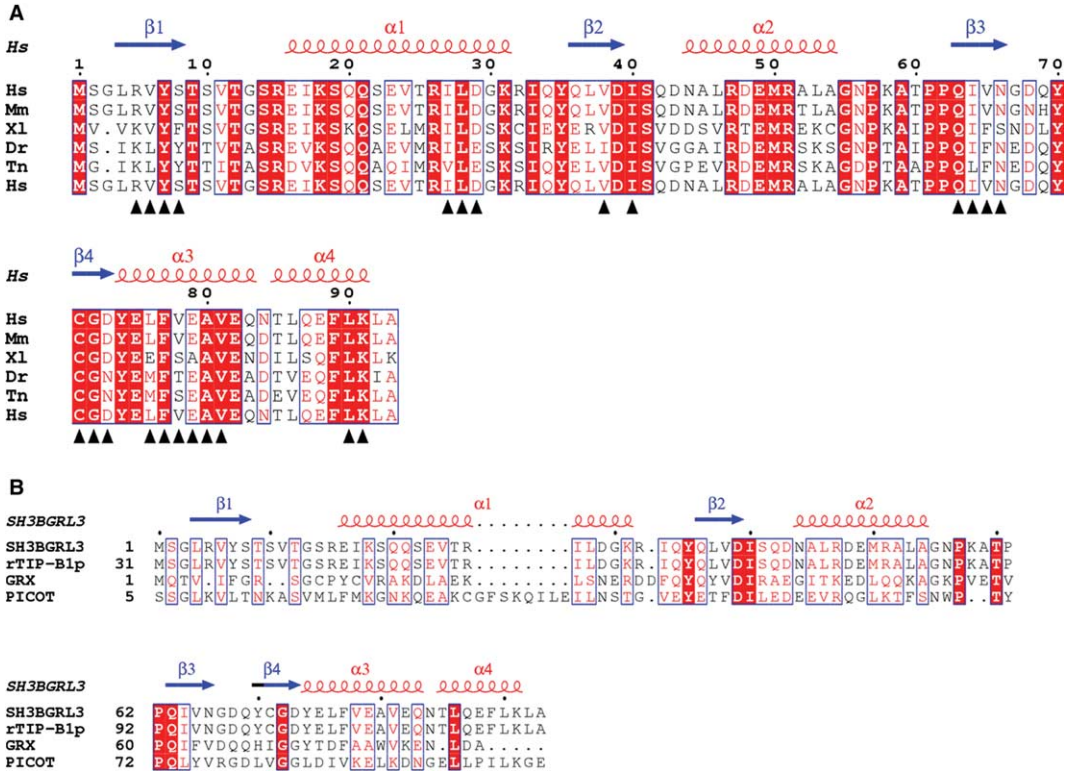

Fig. 2. Structural sequence alignment of (A) isoforms of SH3BGRL3 in different organisms. Dashes introduced for maximum alignment. Hs, *Homo sapiens* (CAI15827); Mm, *Mus musculus* (AAH08110); Xl, *Xenopus laevis* (AAH68879); Dr, *Danio rerio* (AAH49323); Tn, *Tetraodon nigroviridis* (CAG04692). (B) SH3BGRL3, *human SH3BGRL3*; rTIP-B1p, *recombinant TIP-B1*; GRX, *E. coli Glutaredoxin 3*; PICOT, *the second PICOT homology domain of PICOT* (PDB id: 1WIK). The secondary structure of human SH3BGRL3 is indicated above the alignment. Residues identical in all five sequences are colored white in red column and conserved residues are colored red, while the others are in black. The residues that could be observed after ^{1}H–^{2}H exchange experiments are marked at bottom in (A).

3. Results

3.1. Sequence assignment and NMR determination of human SH3BGRL3

Complete backbone and nearly complete (>95%) side chain assignments of residues S2–A93 were made for ^{1}HN, ^{15}N, $^{1}H_{\alpha}$, $^{1}H_{\beta}$, $^{13}C\alpha$, and $^{13}C_{\beta}$. In fact, the recombinant protein contains full length of SH3BGRL3, and an N-terminal Met and a C-terminal his tag, which were not well assigned. All chemical shifts of the resonance assignments have been deposited in BMRB (Accession No. 6152).

The root mean square deviation (r.m.s.d.) for the backbone atoms N, CA, and CO (residues 4–92) was 0.55 Å (Fig. 1A) and for the backbone heavy atoms 1.00 Å. Structural statistics is summarized in Table 1.

3.2. Description of the structure

The resulting structure of SH3BGRL3 (PDB ID, 1SJ6) shares the fold typical to TRX super family [33]. There are four internal β-sheets (4–8, 36–39, 63–66, and 71–73) and four α-helices (16–31, 44–54, 74–83, and 85–91). Strands β1 and β2 are parallel, while others are anti-parallel (Fig. 1B). In ^{1}H–^{2}H exchange experiment, it is intriguing that ^{1}HN of Asp 73 and Leu 76 could be observed because their hydrogen bond donor could not be identified in the usual way (Fig. 2A) (i.e., the hydrogen bonds formed between HN of i + 4 residue and CO of i residue in α-helix). So restraints of these two H-bonds, which could be identified unambiguously by angular orientations of preliminary structures, were not involved in initial structure calculation. In NMR structure of SH3BGRL3, HN of Asp 73 and Leu 76 are hydrogen bonded to OD1 of Asp 73, respectively (Fig. 1C). It is one of the typical 'capping box' motifs in Ncap involving a hydrogen bond between OD1 of Asp and HN of N3 (Leu 76) [34]. And Asp73 is conserved in isoforms of SH3BGRL3 in sequence alignment by PHI- and PSI-BLAST (Fig. 2).

3.3. Structural comparison of human SH3BGRL3 in solution and mouse SH3BGRL3 in crystal state

During the preparation of the manuscript, a crystal structure of mouse SH3BGRL3 was reported [35]. They share 95% identity in sequence (Fig. 2A). The development supports the significance of SH3BGRL3 and provides a good opportunity to compare crystal and solution structures from independent research. The overall folds of SH3BGRL3 structures determined by NMR and X-ray crystallography appear to be very similar (Fig. 3) and the global r.m.s.d. calculated for the backbone atoms (residues 4–92) of the average secondary structures in 20 structures in solution and the X-ray crystal structure is 0.58 Å, which is within the precision of the two structure determinations.

Although solution structure of human SH3BGRL3 and crystal structure of mouse SH3BGRL3 are very similar, there are still significant differences existing between them. A classical type of Ncap interaction in helix involving OG of Ser 14 and HN of Ile 17, which existed in the crystal structure [35], could not be found in NMR structures for the fast exchange characteristics of HN of Ile 17 in ^{1}H–^{2}H exchange experiments (Fig. 3). In structure comparison, the difference reflects the flexibility of loop linking β1 and α1 in solution. Line broadening of Gly 13 by averaging chemical shift could be observed in HSQC, and peaks in other spectra correlated to Gly 13 were much weaker.

3.4. Structure implication for potential binding sites

In backbone relaxation experiments (in supplementary material), T_2s of S14, E16 (~60 ms) and residues between β2

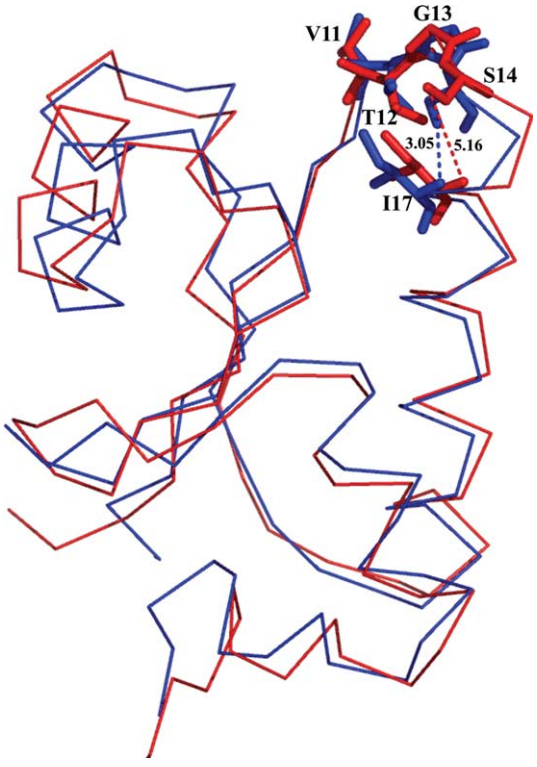

Fig. 3. Structure comparison of one ensemble of solution structure of human SH3BGRL3 (red) and crystal structure of mouse SH3BGRL3 (blue). The side chains of V11, T12, G13, V14 and I17 are shown. The distances between OG of Ser14 and HN of 17 are marked, respectively.

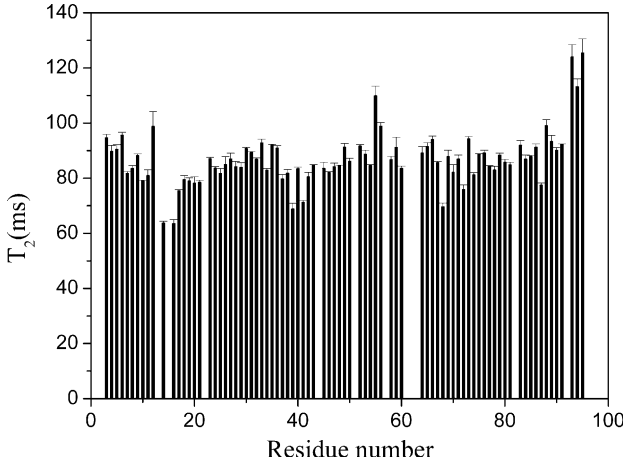

Fig. 4. Plots of T_2 (ms) as a function of residue number of human SH3BGRL3. Only residues whose ^{1}H–^{15}N cross-peaks are resolved enough to permit accurate measurements of their intensities are included.

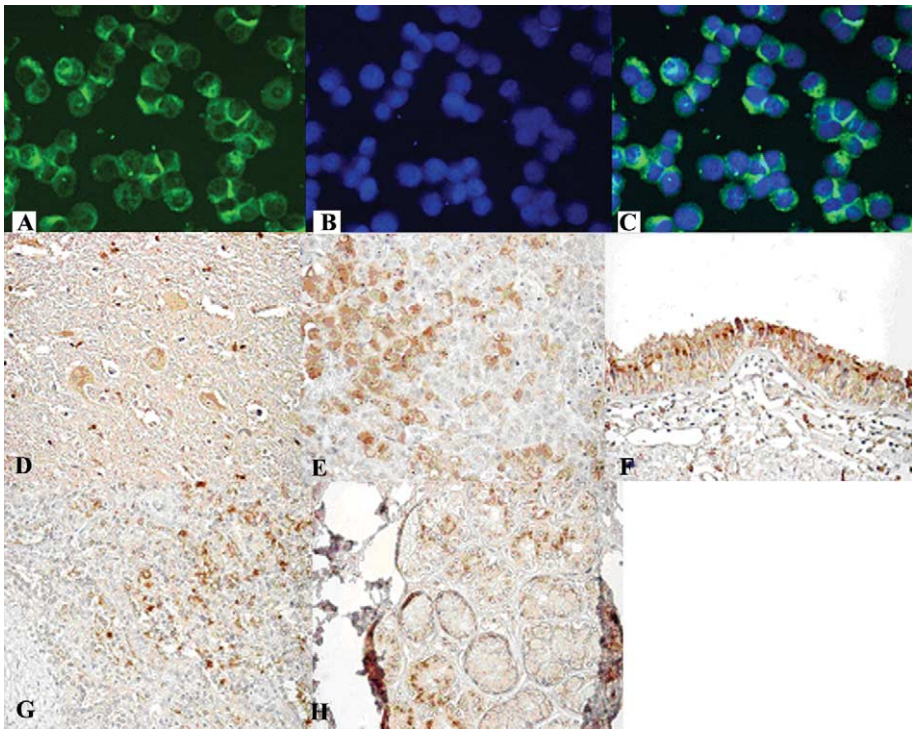

Fig. 5. Cellular localization tissue expression distribution of SH3BGRL3. (A) Immunofluorescent image revealed SH3BGRL3 expression in cytoplasma in NB4 cells. Purified ascites from P8E07 was used as primary antibody and FITC-labeled rabbit-anti-mouse antibody as secondary antibody. This cell was treated with ATRA for 48 h. (B) NB4 cell nuclear was stained with Loftan. (C) Integration of (A) and (B) could demonstrate the cytoplasmic localization in NB4 cell clearly. (D–H) SH3BGRL3 expression in normal tissues, HRP-conjugated goat-anti-mouse IgG was used as secondary antibody and DAB as colorimetrics in color development. (D) Brain, (E) spleen, (F) trachea, (G) pancreas, (H) esophagus.

and α2 smaller than those of other residues (~80–100 ms) (Fig. 4), combined with peaks of Gly 13 and Arg 15 cannot be observed, which indicates that the loop exhibits a conformational exchange in solution. In helix α2, no backbone HN exchange slowly in ^{1}H-^{2}H exchange experiments, which could be explained as 'structure breath' for binding its partner. Conserved positive-charged amino acids in helix α1 (Lys 18, Gln 20, and Gln 21) and α2 (Arg 47 and Arg 51) are notable (Fig. 1B). Although the partner of SH3BGRL3 remains unknown, relaxation experiments, as a whole, suggest that the active sites of SH3BGRL3 are located on the flexible loop connecting β1–α1, helix α1, and helix α2. This speculated active-site location of SH3BGRL3 is consistent with type 1 location in recent report, which is consistent with other TRX-like proteins of TRX superfamily with known structure [36].

3.5. Subcellular localization and tissue distribution of SH3GRL3 in human

For SH3BGRL3 has no nuclear localization signal, nor enzymatic activity site at both sequence and structure level, the subcellular localization could give important hints for its biological meaning. The monoclonal antibody P8E07 was applied to map the expression of the nature of SH3BGRL3 in NB4 and normal human tissues. In NB4 cell, strong cytoplasmic signal and almost no nuclear signal was detected by fluorescence microscopy (Fig. 5A–C). In normal human tissues, SH3BGRL3 protein could be detected in brain, spleen, trachea, pancreas and esophagus with tissue microarray, and revealed to be localized in cytoplasma (Fig. 5D–H).

3.6. Expression of SH3BGRL3 in NB4 cells is upregulated and paralleled with differentiation induced by all-trans retinoic acid

NB4 is a representative APL cell line, and the model of differentiation induced by ATRA has been well established [9]. Studying the gene expression profiling regulation induced by ATRA in NB4 cells, we identified the up-regulation of SH3BGRL3 at mRNA level from early time, and reached the top after treating with ATRA for 12 h (Fig. 6A), as an early event [9], and the real-time quantitative RT-PCR could validate these results (Fig. 6C). Furthermore, Western blot revealed that the protein expression was also up-regulated during this course with similar curve, and reached the top at almost 24 h with 12 h later than gene expression (Fig. 6B). This strongly paralleled with the differentiation effect of NB4 [9].

4. Discussion

In this paper, we present the solution structure of human SH3BGRL3 and its regulated expression in APL Cell line NB4 by ATRA, and we speculate its potential binding site from its structure similarity and relaxation experiments. Structure comparison with other known structures reveals that it belongs to TRX-like family, and its structure is similar to glutaredoxin of *E. coli* [10] and PICOT homology domain 2 of PICOT (PDB 1WIK) [11]. PICOT homology domain also exists in other organisms as a regulatory domain [11,37]. SH3BGRL3, as well as N-terminal domain of PICOT, lacks

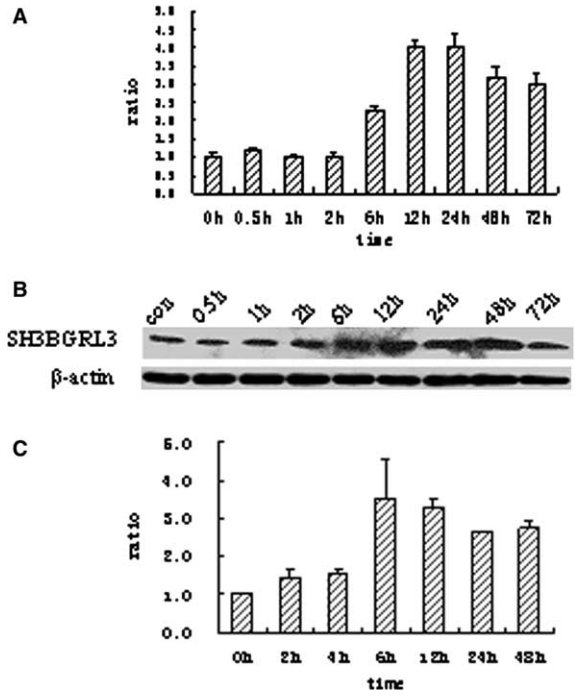

Fig. 6. Expression of SH3BGRL3 in NB4 cells is upregulated and is in agreement with differentiation induced by ATRA. (A) cDNA microarray results indicated the expression level comparing with the control NB4 cell RNA, the expression regulation is shown with the fluorescence intensity ratios of Cy5 versus Cy3-labeled to test and reference mRNA, respectively. (B) Western blot analysis of the SH3BGRL3 protein level. The cell lysates were prepared same as in (A). (C) The real-time RT-PCR analysis of *SH3BGRL3* gene expression in NB4 cells. The reaction and cycling conditions are indicated in the text. The Ct of SH3BGRL3 was normalized with the Ct of GAPDH gene, the expression level was converted with 2 exp(Ct), and non-ATRA treated cells were used as reference. The *x*-axis indicated the ATRA treated time, and *y*-axis in (A) and (C) indicated the expression levels comparing with non-treated cells.

the conserved CXXC motif, which is essential for glutaredoxin enzymatic activity, thus is devoid of the TRX enzyme activity. PICOT is identified in human T lymphocytes as a protein kinase C (PKCϑ) interacting protein. It plays a negative regulatory role in cellular stress response associated with activation of AP-1 and NF-κB. The interaction between PICOT and PKC indicates that the TRX enzyme activity is not indispensable for the interaction between the PKC superfamily and TRX system [11]. It has been found that PKC isoforms are involved in PMA-induced and ATRA-induced pathway [38,39]. These give the hint that SH3BGRL3 may function as a regulator rather than an enzyme in the ATRA-induced pathway through regulating the interaction between TRX system and PKC superfamily. Further work is required to elucidate its physiological role and partner in ATRA-induced pathway.

Several members of TNF pathway regulated by ATRA have been reported; within them, one pathway is related to activation of NF-κB. Activation of NF-κB inhibits TNF-induced apoptosis, which could turn on the transcription of genes that counter the proapoptotic effects of TNF [40]. Posttranslational modified SH3BGRL3 could inhibit the cell lysis induced by TNF-α and play an important role in regulating TNF-induced cascade reaction [4]. So, the ATRA-induced expression of SH3BGRL3 may be explained by activation of TNF-induced NF-κB. This study should provide a basis for further studies of mechanism of human SH3BGRL3 in ATRA-induced and TNF-induced pathway.

Acknowledgments: This work was supported by the Chinese National Fundamental Research Project, Grants G1999075605 and 2002CB713806; the Chinese National Natural Science Foundation, Grants 30270293 and 30121001; the Key Project of the National High Technology Research and Development Program of China, Grants 2002BA711A13 and 2002AA2Z2002; the Pilot Project of the Knowledge Innovation Program of the Chinese Academy of Science, Grant KSCX1-SW-17; and Shanghai Municipal Science and Technology Projects, Grant 034319218.

Appendix A. Supplementary data

Supplementary data associated with this article can be found, in the online version at doi:10.1016/j.febslet.2005.04.011.

References

[1] Mazzocco, M., Arrigo, P., Egeo, A., Maffei, M., Vergano, A., Di Lisi, R., Ghiotto, F., Ciccone, E., Cinti, R., Ravazzolo, R. and Scartezzini, P. (2001) A novel human homologue of the SH3BGR gene encodes a small protein similar to glutaredoxin 1 of *Escherichia coli*. Biochem. Biophys. Res. Commun. 285, 540–545.
[2] Egeo, A., Mazzocco, M., Arrigo, P., Vidal-Taboada, J.M., Oliva, R., Pirola, B., Giglio, S., Rasore-Quartino, A. and Scartezzini, P. (1998) Identification and characterization of a new human gene encoding a small protein with high homology to the proline-rich region of the SH3BGR gene. Biochem. Biophys. Res. Commun. 247, 302–306.
[3] Mazzocco, M., Maffei, M., Egeo, A., Vergano, A., Arrigo, P., Di Lisi, R., Ghiotto, F. and Scartezzini, P. (2002) The identification of a novel human homologue of the SH3 binding glutamic acid-rich (SH3BGR) gene establishes a new family of highly conserved small proteins related to thioredoxin Superfamily. Gene 291, 233–239.
[4] Berleth, E.S., Nadadur, S., Henn, A.D., Eppolito, C., Shiojiri, S., Gurtoo, H.L., Ehrke, M.J. and Mihich, E. (1999) Identification, characterization, and cloning of TIP-B1, a novel protein inhibitor of tumor necrosis factor-induced lysis. Cancer Res. 59, 5497–5506.
[5] Berleth, E.S., Masso-Welch, P.A., Kazim, L.A., Ip, M.M., Mihich, E. and Ehrke, M.J. (2000) A novel tumor necrosis factor-alpha inhibitory protein, TIP-B1. Int. J. Immunopharmacol. 22, 1137–1142.
[6] Henn, A.D., Berleth, E.S., Mihich, E. and Ehrke, M.J. (2001) Changes in cytosolic and membrane TNF inhibitory protein-B1 (TIP-B1) levels associated with protection from TNF-induced cytotoxicity. FASEB J. 15, 1315–1317.
[7] Berleth, E.S., Masso-Welch, P.A., Kazim, L.A., Ip, M.M., Mihich, E. and Ehrke, M.J. (2001) Expression, tissue distribution, and cellular localization of the antiapoptotic TIP-B1 protein. J. Leukoc. Biol. 69, 995–1005.
[8] Seo, J., Kim, M. and Kim, J. (2000) Identification of novel genes differentially expressed in PMA-induced HL-60 cells using cDNA microarrays. Mol. Cells 10, 733–739.
[9] Liu, T.X., Zhang, J.W., Tao, J., Zhang, R.B., Zhang, Q.H., Zhao, C.J., Tong, J.H., Lanotte, M., Waxman, S., Chen, S.J., Mao, M., Hu, G.X., Zhu, L. and Chen, Z. (2000) Gene expression networks underlying retinoic acid-induced differentiation of acute promyelocytic leukemia cells. Blood 96, 1496–1504.
[10] Nordstrand, K., Sandstrom, A., Aslund, F., Holmgren, A., Otting, G. and Berndt, K.D. (2000) NMR structure of oxidized glutaredoxin 3 from *Escherichia coli*. J. Mol. Biol. 303, 423–432.
[11] Witte, S., Villalba, M., Bi, K., Liu, Y., Isakov, N. and Altman, A. (2000) Inhibition of the c-Jun N-terminal kinase/AP-1 and NF-kappaB pathways by PICOT, a novel protein kinase C-interacting protein with a thioredoxin homology domain. J. Biol. Chem. 275, 1902–1909.

[12] Mao, M., Yu, M., Tong, J.H., Ye, J., Zhu, J., Huang, Q.H., Fu, G., Yu, L., Zhao, S.Y., Waxman, S., Lanotte, M., Wang, Z.Y., Tan, J.Z., Chan, S.J. and Chen, Z. (1996) RIG-E, a human homolog of the murine Ly-6 family, is induced by retinoic acid during the differentiation of acute promyelocytic leukemia cell. Proc. Natl. Acad. Sci. USA 93, 5910–5914.
[13] Zheng, P.Z., Wang, K.K., Zhang, Q.Y., Huang, Q.H., Du, Y.Z., Zhang, Q.H., Xiao, D.K., Shen, S.H., Eveno, E., Zhao, C.J., Chen, Y.L., Fan, H.Y., Waxman, S., Auffray, C., Jin,G., Chen, S.J., Chen, Z. and Zhang, J. (2005). Systems analysis of transcriptome and proteome in retinoic acid/arsenic trioxide combination-induced cell differentiation/apoptosis of acute promyelocytic leukemia. Proc. Natl. Acad. Sci. USA (in press).
[14] Bax, A., Ikura, M., Kay, L.E., Torchia, D.A. and Tschudin, R. (1990) Comparison of different modes of two-dimensional reverse correlation NMR for the study of proteins. J. Magn. Reson. 86, 304–318.
[15] Muhandiram, D.R. and Kay, L.E. (1994) Gradient-enhanced triple resonance three-dimensional NMR experiments with improved sensitivity. J. Magn. Reson. B103, 203–216.
[16] Clubb, R.T., Thanabal, V. and Wagner, G. (1992) A constant-time 3-dimensional tripleresonance pulse scheme to correlate intraresidue H-1(N), N-15, and C-13(′) chemical shifts in N-15-C-13-labeled proteins. J Magn. Reson. 97, 213–217.
[17] Grzesiek, S. and Bax, A. (1992) Correlating backbone amide and side chain resonances in larger proteins by multiple relayed triple resonance NMR. J. Am. Chem. Soc. 114, 6291–6293.
[18] Grzesiek, S. and Bax, A. (1992) An efficient experiment for sequential backbone assignment of medium-sized isotopically enriched proteins. J. Magn. Reson. 99, 201–207.
[19] Logan, T.M., Olejniczak, E.T., Xu, R.X. and Fesik, S.W. (1993) A general method for assigning NMR spectra of denatured proteins using 3D HC(CO)NH-TOCSY triple resonance experiments. J. Biomol. NMR 3, 225–231.
[20] Bax, A., Clore, G.M. and Gronenborn, A.M. (1990) ^{1}H–^{1}H correlation via isotropic mixing of ^{13}C magnetization, a new three-dimensional approach for assigning ^{1}H and ^{13}C spectra of ^{13}C enriched proteins. J. Magn. Reson. 88, 425–431.
[21] Bax, A., Clore, G.M., Driscoll, P.C., Gronenborn, A.M., Ikura, M. and Kay, L.E. (1990) Practical aspects of proton-carbon-carbon-proton three-dimensional correlation spectroscopy of ^{13}C labeled proteins. J. Magn. Reson. 87, 620–627.
[22] Grzesiek, S. and Bax, A. (1993) Amino acid type determination in the sequential assignment procedure of uniformly ^{13}C/^{15}N-enriched proteins. J. Biomol. NMR 3, 185–204.
[23] Yamazaki, T., Formankay, J.D. and Kay, L.E. (1993) 2-Dimensional NMR experiments for correlating C-13-beta and H-1-delta/epsilon chemical-shifts of aromatic residues in C-13-labeled proteins via scalar couplings. J. Am. Chem. Soc. 115, 11054–11055.
[24] Wishart, D.S. and Sykes, B.D. (1994) The ^{13}C chemical-shift index: a simple method for the identification of protein secondary structure using ^{13}C chemical-shift data. J. Biomol. NMR 4, 171–180.
[25] Zuiderweg, E.R.P. and Fesik, S.W. (1989) Heteronuclear three-dimensional NMR spectroscopy of the inflammatory protein C5a. Biochemistry 28, 2387–2391.
[26] Goddard, T.D. and Kneller, D.G. (2002) Sparky 3. University of California, SF.
[27] Brunger, A.T., Adams, P.D., Clore, G.M., Delano, W.L., Gros, P., Grosse-Kunstleve, R.W., Jiang, J.S., Kuszewski, J., Nilges, M., Pannu, N.S., Read, R.J., Rice, L.M., Simonson, T. and Warren, G.L. (1998) Crystallography & NMR system: a new software suite for macromolecular structure determination. Acta Crystallogr. D 54, 905–921.
[28] Stein, E.G., Rice, L.M. and Brunger, A.T. (1997) Torsion-angle molecular dynamics as a new efficient tool for NMR. J. Magn. Reson. 124, 154–164.
[29] Farrow, N.A., Muhandiram, R., Singer, A.U., Pascal, S.M., Kay, C.M., Gish, G., Shoelson, S.E., Pawson, T., Forman-Kay, J.D. and Kay, L.E. (1994) Backbone dynamics of a free and phosphopeptide-complexed Src homology 2 domain studied by ^{15}N NMR relaxation. Biochemistry 33, 5984–6003.
[30] Kononen, J., Bubendorf, L., Kallioniemi, A., Barlund, M., Schraml, P., Leighton, S., Torhorst, J., Mihatsch, M.J., Sauter, G. and Kallioniemi, O.P. (1998) Tissue microarrays for high-throughput molecular profiling of tumor specimens. Nat. Med. 4, 844–847.
[31] Chen, G.Q., Shen, Z.X., Wu, F., Han, J.Y., Miao, J.M., Zhong, H.J., Li, X.S., Zhao, J.Q., Zhu, J., Fang, Z.W., Chen, S.J., Chen, Z. and Wang, Z.Y. (1996) Pharmacokinetics and efficacy of low-dose all-*trans* retinoic acid in the treatment of acute promyelocytic leukemia. Leukemia. 10, 825–828.
[32] Laskowski, R.A., Rullmannn, J.A., MacArthur, M.W., Kaptein, R. and Thornton, J.M. (1996) AQUA and PROCHECK-NMR: programs for checking the quality of protein structures solved by NMR. J. Biomol. NMR 8, 477–486.
[33] Martin, J.L. (1995) Thioredoxin – a fold for all reasons. Structure 3, 245–250.
[34] Aurora, R. and Rose, G.D. (1998) Helix capping. Protein Sci. 7, 21–38.
[35] Nardini, M., Mazzocco, M., Massaro, A., Maffei, M., Vergano, A., Donadini, A., Scartezzini, P. and Bolognesi, M. (2004) Crystal structure of the glutaredoxin-like protein SH3BGRL3 at 1.6 Angstrom resolution. Biochem. Biophys. Res. Commun. 318, 470–476.
[36] Qi, Y. and Grishin, N.V. (2005) Structural classification of thioredoxin-like fold proteins. Proteins 58, 376–388.
[37] Rahlfs, S., Fischer, M. and Becker, K. (2001) *Plasmodium falciparum* possesses a classical glutaredoxin and a second, glutaredoxin-like protein with a PICOT homology domain. J. Biol. Chem. 276, 37133–37140.
[38] Kambhampati, S., Li, Y., Verma, A., Sassano, A., Majchrzak, B., Deb, D.K., Parmar, S., Giafis, N., Kalvakolanu, D.V., Rahman, A., Uddin, S., Minucci, S., Tallman, M.S., Fish, E.N. and Platanias, L.C. (2003) Activation of protein kinase C delta by all-*trans*-retinoic acid. J. Biol. Chem. 278, 32544–32551.
[39] Hewson, C.A., Edbrooke, M.R. and Johnston, S.L. (2004) PMA induces the MUC5AC respiratory mucin in human bronchial epithelial cells, via PKC, EGF/TGF-alpha, Ras/Raf, MEK, ERK and Sp1-dependent mechanisms. J. Mol. Biol. 344, 683–695.
[40] Witcher, M., Ross, D.T., Rousseau, C., Deluca, L. and Miller Jr., W.H. (2003) Synergy between all-*trans* retinoic acid and tumor necrosis factor pathways in acute leukemia cells. Blood 102, 237–245.